

Growth Suppression of Cancer Spheroids With Mutated *KRAS* by
Low-toxicity Compounds from Natural Products

SAYURI HASHIMOTO¹, MASAYOSHI NAGAI¹, KENSUKE NISHI^{1,2}, SHUHEI
ISHIKURA^{1,3}, KAZUHIKO NAKABAYASHI⁴, RYO YAZAKI⁵, TAKASHI OHSHIMA⁵,
MASAHIKO SUENAGA⁶, SENJI SHIRASAWA^{1,3} and TOSHIYUKI TSUNODA^{1,3}

*Departments of ¹Cell Biology, Faculty of Medicine, and ³Central Research
Institute for Advanced Molecular Medicine, Fukuoka University, Fukuoka,
Japan;*

*²Section of Otolaryngology, Department of Medicine, Fukuoka Dental College,
Fukuoka, Japan;*

*⁴Department of Maternal-Fetal Biology, National Center for Child Health and
Development, Tokyo, Japan;*

*⁵Graduate School of Pharmaceutical Sciences, and ⁶Department of Chemistry,
Graduate School of Science, Kyushu University, Fukuoka, Japan*

Correspondence to: Toshiyuki Tsunoda, MD, Ph.D., Department of Cell Biology,
Faculty of Medicine Fukuoka University, 7-45-1 Nanakuma, Jonan-ku, Fukuoka 814-
0180, Japan. Tel: +81 928011011, Fax: +81 928643865, e-mail: tsunoda@fukuoka-u.ac.jp

Key Words:

Colorectal cancer, *KRAS*, 3D floating culture, Natural products

Running title: STAR3 Induces Growth Suppression of Colorectal Cancer Spheroids

Appropriate Section: Experimental

Date of Submission: 22 May, 2021

Abstract

Background/Aim: Among compounds from natural products selectively suppressing the growth of cancer spheroids, which have mutant (mt) KRAS, NP910 was selected and its derivatives explored. Materials and Methods: The area of HKe3 spheroids expressing wild type (wt) KRAS (HKe3-wtKRAS) and mtKRAS (HKe3-mtKRAS) were measured in three-dimensional floating (3DF) cultures treated with 18 NP910 derivatives. The 50% cell growth inhibition (GI50) was determined by long-term 3DF (LT3DF) culture and nude mice assay. Results: We selected NP882 (named STAR3) as the most effective inhibitor of growth of HKe3-mtKRAS spheroids with the least toxicity among NP910 derivatives. GI50s of STAR3 in LT3DF and nude mice assay were 6 μ M and 30.75 mg/kg, respectively. However, growth suppression by STAR3 was observed in 50% of cell lines independent of KRAS mutation, suggesting that the target of STAR3 was not directly associated with KRAS mutation and KRAS-related signals. Conclusion: STAR3 is a low-toxicity compound that inhibits growth of certain tumour cells.

KRAS is the most frequently mutated oncogene among human cancers (1), with high rates of activating missense mutations in pancreatic cancers (86 to 96%) (2), in colorectal cancers (CRC) (40 to 54%), and in non–small cell lung cancer (NSCLC) (15 to 20%) (3, 4). Once activated, mutated RAS remains "on" persistently, thereby enhancing down-stream signaling and leading tumourigenesis. Recently, AMG510, which targets specifically *KRAS* G12C mutant, was developed and was found to be effective in clinical trials in some patients with NSCLC (5). However, the *KRAS* G12C mutation occur in about 13% of NSCLCs (6, 7), in 3 to 5% of CRCs, and in 1 to 2% of various other solid cancers (3) (5, 8-10). Therefore, the range of use of AMG510 is limited, and the *KRAS* mutation is still an "undruggable" target.

Canonical anticancer agents, including alkylating drugs, platinum compounds, antimetabolites, topoisomerase inhibitors, and microtubule inhibitors, are highly toxic and cause serious side effects such as myelosuppression (11, 12). Recently, molecularly targeted drugs are expected to be the new drugs with low toxicity (13); however, drug resistance is unavoidable (14). Therefore, new types of compounds are indispensable for cancer treatment.

Recently, we screened genes that were upregulated by mtKRAS in a three-dimensional (3D) matrigel culture and found that the phosphodiesterase 4B (PDE4B) levels were higher in clinical tumour samples from CRC patients in comparison to

those from healthy control (15). We examined several PDE4 inhibitors, such as pan PDE4 inhibitor, resveratrol, and PDE4 selective inhibitor, apremilast (16, 17), revealing that these compounds are selective for cancer spheroids with mtKRAS, and exhibit high efficacy and low toxicity. Notably, resveratrol, which has similar PDE4-inhibitory activity to that of rolipram (16), is present in various natural products, suggesting that some compounds from natural products will become low-toxicity anticancer agents.

To screen compounds from natural products, we established 3D floating (3DF) culture using HKe3-wtKRAS (normal model) and HKe3-mtKRAS (cancer model) spheroids. Using this system as pilot screening, we identified a 5-bromouridine (BrUrd) (18); uridine derivatives may be able to target HKe3-mtKRAS spheroids selectively and may exhibit low-level toxicity to wtKRAS.

This study, utilized natural product libraries from RIKEN Natural Products Depository (NPDepo) and found several core compounds, including NP910 (19) and explored the efficacy of NP910 derivatives using 3DF culture. We selected NP882 (19) as lead compound and further examined its properties.

Materials and Methods

Compounds. Compounds library from natural products were kindly provided by RIKEN NPDepo (Saitama, Japan). Chemical distances were determined by the Jaccard

similarity index (20).

Cell culture. HKe3, HKe3-wtKRAS, and HKe3-mtKRAS cultures were established and maintained as described previously (21, 22). DLD-1, SW620, SW837, A549, MIA PaCa2, Hs766T, HepG2, HEC1-B, CCK-81, Hs700T, SK-M EL-28, A498, DU145, MCF-7, HeLa, Caov-3 cells were purchased from the American Type Culture Collection (ATCC, Manassas, VA, USA) and maintained at 37°C in 5% CO₂ atmosphere in Dulbecco's modified Eagle's medium supplemented with 10% fetal bovine serum and 1% penicillin/streptomycin as described previously (21, 22).

Short-term 3D floating cell culture. Cells were seeded in 96-well plates with round-bottom and ultralow attachment surfaces (product number 7007; Corning Inc., Corning, NY, USA) and treated with a drug at day 0. Cells were maintained at 37°C in 5% CO₂ atmosphere as described previously (18, 22, 23).

Long-term 3D floating cell culture. Cells were seeded in 96-well plates and treated with a drug at day 0. The drug added every three days and the area of spheroids was measured every three to four days until day 27 as previously described (18).

Measurement of area of spheroids. Photomicrographs of cells were taken and analyzed using an IN Cell Analyzer 1000 (GE Healthcare, Little Chalfont, UK) and IN Cell Developer Toolbox (GE Healthcare). The relative growth rate was calculated from a comparison of the area of control spheroids at day three.

Assay for tumourigenicity. Four-week-old female SHO mice (Crlj:SHO-Prkdc^{scid}Hr^{hr}) were purchased from Charles River Laboratories (Yokohama, Japan). Cells for implantation were trypsinized and re-suspended in a 1:1 mixture of phosphate-buffered saline and Matrigel (BD Bioscience, Bedford, MA, USA). A 100 µl volume containing 1.5×10^6 HCT116 cells was subcutaneously injected into the flank of mice as described previously (17).

Statistical analyses. All experiments were performed in triplicate. Data are presented as means \pm standard deviations. Statistical analyses were performed using unpaired two-tailed Student's *t*-test in Microsoft Excel. *p*-Values of less than 0.05 were considered statistically significant.

Results

NP910 derivatives inhibit the growth of HKe3-mtKRAS cells grown in 3DF cultures.

During the first screening of compounds from natural products, NP910 was identified as a candidate drug that inhibits the growth of HKe3-mtKRAS spheroids but not HKe3-wtKRAS spheroids (data not shown). Eighteen NP910 derivatives were selected from RIKEN libraries of natural products using chemical distance (11) (Table I). Cells were treated with 16.6 μ M and 50.0 μ M of 18 NP910 derivatives in 3DF culture to examine the effects of NP910 derivatives on cell proliferation. The area of HKe3-mtKRAS spheroids treated with 16.6 μ M of NP882 at day 6 was 1.27-fold larger in comparison to that of HKe3-wtKRAS spheroids treated with DMSO at day 6 (Figure 1A), suggesting that NP882 displays the highest efficacy for suppressing the growth of cancer cells. The area of HKe3-mtKRAS spheroids treated with 50.0 μ M of NP910, NP770, NP917, and NP882 at day 6, was 1.19-, 0.11-, 0.16-, and 0.86-fold smaller in comparison to that of HKe3-wtKRAS spheroids treated with DMSO at day 6, respectively (Figure 1B). The area of HKe3-wtKRAS spheroids treated with 16.6 μ M of NP910, NP770, NP917, and NP882 at day 6 were 1.53-, 1.68-, 1.99-, and 2.01-fold larger in comparison to that of HKe3-wtKRAS spheroids treated with DMSO at day 6, respectively (Figure 1A), suggesting that NP917 and NP882 will show the lowest toxicity for normal cells. To select the best compounds from these derivatives, we have scored the toxicity in normal model (Hke3-wtKRAS) and the efficacy of growth suppression in caner model in low or high dose. Furthermore, we added the growth

rate from day3 to day6 in cancer model for scoring (Table II). These results together suggest that NP882 (named STAR3) is a good candidate for further analyses.

The long-term effects of STAR3 for HKe3- wtKRAS and mtKRAS spheroids. A long-term 3DF culture was established to determine the cytotoxicity of STAR3 during long-term exposure. The area of HKe3-wtKRAS spheroids treated with STAR3 at day 27 was similar to DMSO control (Figure 2A), suggesting that none of the drugs is cytotoxic to cells with wtKRAS. Treatment of HKe3-mtKRAS spheroids by serially-diluted STAR3 showed that the concentration required to achieve a 50% maximal inhibition in cell proliferation is approximately 6 μ M (Figure 2B).

Effect of STAR3 on in vivo tumourigenicity of human colorectal cancer HCT116 cells.

HCT116 cells were injected subcutaneously into the nude mice to address the effects of STAR3 on tumourigenicity of HCT116 cells, STAR3 was administered on day 0. In control mice, tumour volume was 2362 mm³ on day 7. In contrast, in mice treated with 10mg/kg, 40mg/kg and 50mg/kg STAR3 tumour volume was 1985 mm³, 750 mm³, and 514 mm³, at day 7, respectively(Figure 3). GI50 was 30.75 mg/kg. HCT116 cell tumour volume was dramatically reduced in in mice treated with STAR3 compared to those administered DMSO, suggesting that STAR3 inhibits tumour growth *in vivo*.

Efficacy of STAR3 on several cell lines. To examine the efficacy of STAR3 against other cell lines, 3DFCs were performed using 2, 6, 18, 54, and 162 (high concentration) μM of STAR3 (Table III). The number of cell lines in which STAR3 suppressed cell growth was 9 (50%). The number of mtKRAS cell lines whose growth was suppressed by STAR3, was 6 (60%). On the other hand, the number of wtKRAS cell lines whose growth was suppressed by STAR3 was 3 (37.5%). However, One-tailed Fisher's exact test did not show any significant difference between mtKRAS and wtKRAS cell lines. These results suggest that the target of STAR3 is not closely associated with KRAS-related signals.

Discussion

In this study, we identified STAR3 as a potent drug for cancer with mtKRAS. In long-term 3DFC, GI50 was $6\mu\text{M}$, and drug resistance was not observed. Furthermore, STAR3 showed low toxicity and suppressed the growth of mtKRAS CRC *in vivo*. However, STAR3 was not effective in all cancer cell lines with or without mtKRAS, suggesting that the direct target is not associated with KRAS-related driver genes. There is a possibility that STAR3 will act through KRAS-unrelated genes, which are specific for cell lines. Identification of targets of STAR3 is needed for determining

biomarkers and further developing STAR3.

Recent studies have reported the certain natural compounds that are effective against the KRAS-linked up-stream and down-stream signaling pathways that are directly or indirectly linked with cell proliferation, division, and apoptosis (24, 25). We are now developing another compound (named STAR2) that shows low toxicity, and is effective against all mtKRAS cells.

Conflicts of Interest

The authors declare no competing interests.

Authors' Contributions

S.H., M.N., K.N. and T.T. performed experiments, analysed the data, and wrote a manuscript draft. S.I., K.N., R.Y., and M.S. participated in the study design, data collection, and analysis. T.O. and S.S. conceived the idea and designed the study, interpreted the data, provided important intellectual content, and obtained the final approval of the submitted manuscript.

Acknowledgements

The Authors would like to thank Yuriko Isoyama and Yumiko Hirose for their technical assistance. This work was supported by Grant-in-Aid for Scientific Research (C) (KAKENHI, Grant Number 15K06847, 18K07215) from the Ministry of Education, Culture, Sports, Science, and Technology (MEXT) of Japan and the Fukuoka

References

- 1 Colicelli J: Human ras superfamily proteins and related gtpases. *Sci STKE* 2004(250): Re13, 2004. PMID: 15367757. DOI: 10.1126/stke.2502004re13.
- 2 Biankin AV, Waddell N, Kassahn KS, Gingras MC, Muthuswamy LB, Johns AL, Miller DK, Wilson PJ, Patch AM, Wu J, Chang DK, *et al.*: Pancreatic cancer genomes reveal aberrations in axon guidance pathway genes. *Nature* 491(7424): 399-405, 2012. PMID: 15367757. DOI: 10.1038/nature11547.
- 3 Neumann J, Zeindl-Eberhart E, Kirchner T and Jung A: Frequency and type of kras mutations in routine diagnostic analysis of metastatic colorectal cancer. *Pathol Res Pract* 205(12): 858-862, 2009. PMID: 19679400. DOI: 10.1016/j.prp.2009.07.010.
- 4 Comprehensive molecular profiling of lung adenocarcinoma. *Nature* 511(7511): 543-550, 2014. PMID: 25079552. DOI: 10.1038/nature13385.
- 5 Canon J, Rex K, Saiki AY, Mohr C, Cooke K, Bagal D, Gaida K, Holt T, Knutson CG, Koppada N, Lanman BA, *et al.*: The clinical kras(g12c) inhibitor amg 510 drives anti-tumour immunity. *Nature* 575(7781): 217-223, 2019. PMID: 31666701. DOI: 10.1038/s41586-019-1694-1.
- 6 Biernacka A, Tsongalis PD, Peterson JD, de Abreu FB, Black CC, Gutmann EJ, Liu X, Tafe LJ, Amos CI and Tsongalis GJ: The potential utility of re-mining results of somatic mutation testing: Kras status in lung adenocarcinoma. *Cancer Genet* 209(5): 195-198, 2016. PMID: 27068338. DOI: 10.1016/j.cancergen.2016.03.001.
- 7 Stephen AG, Esposito D, Bagni RK and McCormick F: Dragging ras back in the ring. *Cancer Cell* 25(3): 272-281, 2014. PMID: 24651010. DOI: 10.1016/j.ccr.2014.02.017.
- 8 Jones RP, Sutton PA, Evans JP, Clifford R, McAvoy A, Lewis J, Rousseau A, Mountford R, McWhirter D and Malik HZ: Specific mutations in kras codon 12 are associated with worse overall survival in patients with advanced and recurrent colorectal cancer. *Br J Cancer* 116(7): 923-929, 2017. PMID: 28208157. DOI: 10.1038/bjc.2017.37.
- 9 Wiesweg M, Kasper S, Worm K, Herold T, Reis H, Sara L, Metzenmacher M, Abendroth A, Darwiche K, Aigner C, Wedemeyer HH, *et al.*: Impact of ras mutation subtype on clinical outcome—a cross-entity comparison of patients with advanced non-small cell lung cancer and colorectal cancer. *Oncogene* 38(16): 2953-2966, 2019. PMID: 30568222. DOI: 10.1038/s41388-018-0634-0.
- 10 Zhou L, Baba Y, Kitano Y, Miyake K, Zhang X, Yamamura K, Kosumi K, Kaida T, Arima K, Taki K, Higashi T, *et al.*: Kras, braf, and pik3ca mutations, and patient prognosis in 126

- pancreatic cancers: Pyrosequencing technology and literature review. *Med Oncol* *33(4)*: 32, 2016. PMID: 26927447. DOI: 10.1007/s12032-016-0745-9.
- 11 Oun R, Moussa YE and Wheate NJ: The side effects of platinum-based chemotherapy drugs: A review for chemists. *Dalton Trans* *47(19)*: 6645-6653, 2018. PMID: 29632935. DOI: 10.1039/c8dt00838h.
 - 12 Friberg LE, Henningson A, Maas H, Nguyen L and Karlsson MO: Model of chemotherapy-induced myelosuppression with parameter consistency across drugs. *J Clin Oncol* *20(24)*: 4713-4721, 2002. PMID: 12488418. DOI: 10.1200/jco.2002.02.140.
 - 13 Chari RV: Targeted cancer therapy: Conferring specificity to cytotoxic drugs. *Acc Chem Res* *41(1)*: 98-107, 2008. PMID: 17705444. DOI: 10.1021/ar700108g.
 - 14 Pérez-Herrero E and Fernández-Medarde A: Advanced targeted therapies in cancer: Drug nanocarriers, the future of chemotherapy. *Eur J Pharm Biopharm* *93(52-79)*, 2015. PMID: 25813885. DOI: 10.1016/j.ejpb.2015.03.018.
 - 15 Tsunoda T, Ota T, Fujimoto T, Doi K, Tanaka Y, Yoshida Y, Ogawa M, Matsuzaki H, Hamabashiri M, Tyson DR, Kuroki M, *et al.*: Inhibition of phosphodiesterase-4 (pde4) activity triggers luminal apoptosis and akt dephosphorylation in a 3-d colonic-crypt model. *Mol Cancer* *11(46)*, 2012. PMID: 22830422. DOI: 10.1186/1476-4598-11-46.
 - 16 Luo H, Umebayashi M, Doi K, Morisaki T, Shirasawa S and Tsunoda T: Resveratrol overcomes cellular resistance to vemurafenib through dephosphorylation of akt in braf-mutated melanoma cells. *Anticancer Res* *36(7)*: 3585-3589, 2016. PMID: 27354627.
 - 17 Nishi K, Luo H, Ishikura S, Doi K, Iwaihara Y, Wills L, Baillie GS, Sakata T, Shirasawa S and Tsunoda T: Apremilast induces apoptosis of human colorectal cancer cells with mutant kras. *Anticancer Res* *37(7)*: 3833-3839, 2017. PMID: 28668883. DOI: 10.21873/anticancerres.11762.
 - 18 Luo H, Nishi K, Ishikura S, Swain A, Morishige N, Yazaki R, Ohshima T, Shirasawa S and Tsunoda T: Growth suppression of human colorectal cancer cells with mutated kras by 3-deaza-cytarabine in 3d floating culture. *Anticancer Res* *38(7)*: 4247-4256, 2018. DOI: 10.21873/anticancerres.12721.
 - 19 http://www.cbrg.riken.jp/npedia/kw_search.php
 - 20 Levandowsky M and Winter D: Distance between sets. *Nature* *234(34)*, 1971. PMID: 29970558. DOI: 10.1038/234034a0.
 - 21 Shirasawa S, Furuse M, Yokoyama N and Sasazuki T: Altered growth of human colon cancer cell lines disrupted at activated ki-ras. *Science* *260(5104)*: 85-88, 1993. PMID: 8465203. DOI: 10.1126/science.8465203.
 - 22 Tsunoda T, Ishikura S, Doi K, Iwaihara Y, Hidesima H, Luo H, Hirose Y and Shirasawa S: Establishment of a three-dimensional floating cell culture system for screening drugs targeting kras-mediated signaling molecules. *Anticancer Res* *35(8)*: 4453-4459, 2015. PMID: 26168486.
 - 23 Tsunoda T, Takashima Y, Fujimoto T, Koyanagi M, Yoshida Y, Doi K, Tanaka Y, Kuroki M,

- Sasazuki T and Shirasawa S: Three-dimensionally specific inhibition of DNA repair-related genes by activated kras in colon crypt model. *Neoplasia* *12(5)*: 397-404, 2010. PMID: 20454511. DOI: 10.1593/neo.10170.
- 24 Niloy MS, Shakil MS, Alif MMH and Rosengren RJ: Using natural compounds to target kras mutated non-small cell lung cancer. *Curr Med Chem*, 2021. PMID: 33645474. DOI: 10.2174/0929867328666210301105856.
- 25 Hashemi S, Sharifi A, Zareei S, Mohamedi G, Biglar M and Amanlou M: Discovery of direct inhibitor of kras oncogenic protein by natural products: A combination of pharmacophore search, molecular docking, and molecular dynamic studies. *Res Pharm Sci* *15(3)*: 226-240, 2020. PMID: 33088323. DOI: 10.4103/1735-5362.288425.

Figures and Figure legends

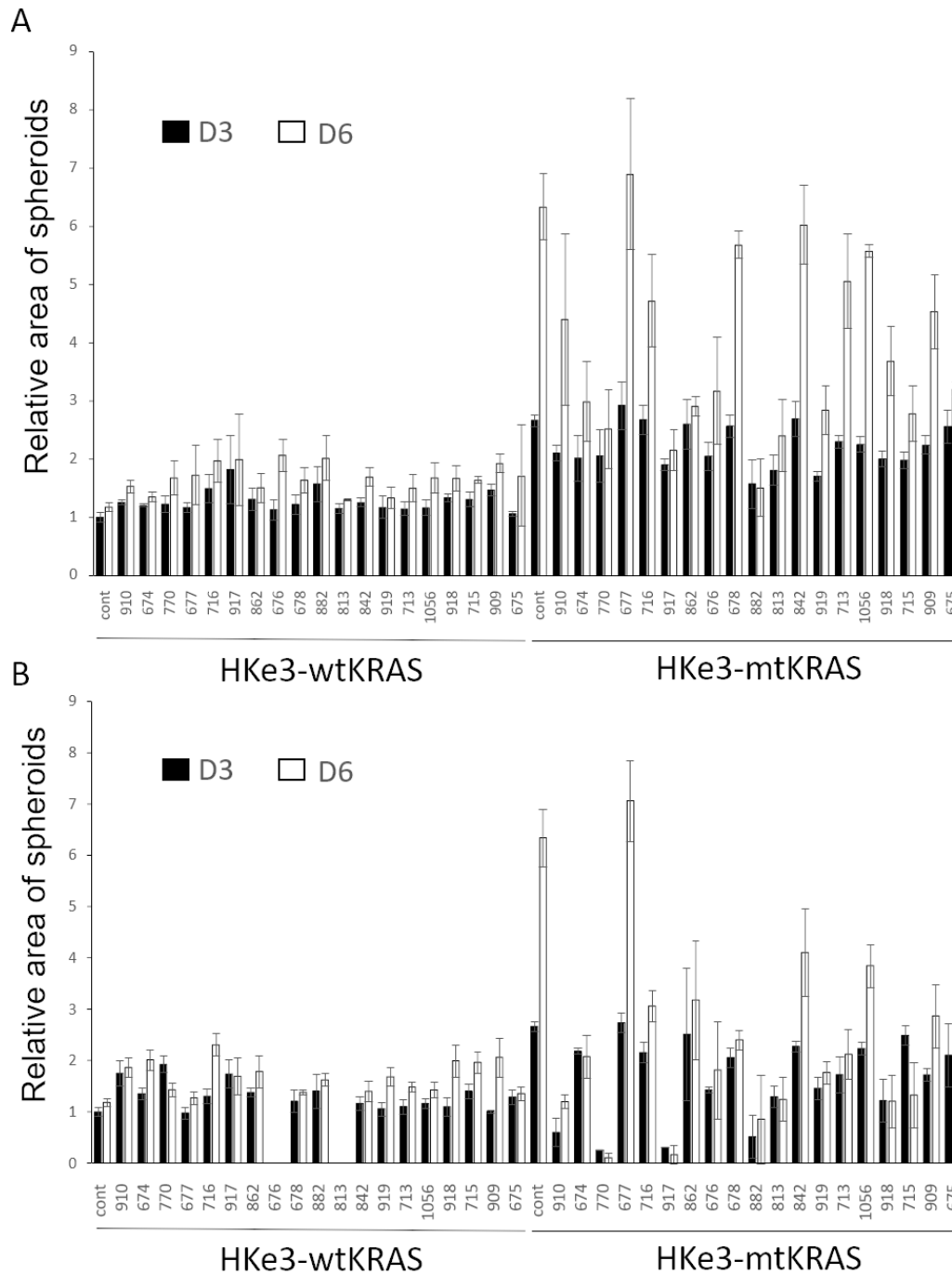
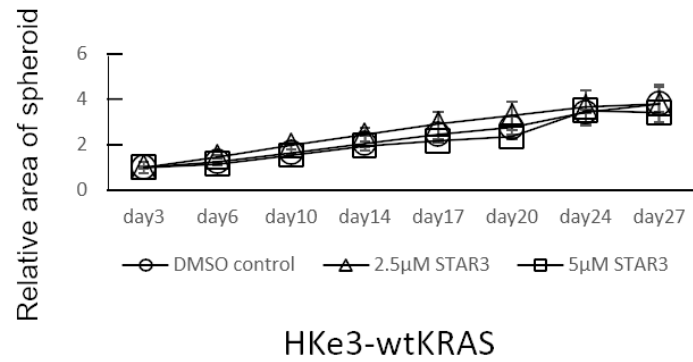


Figure 1. NP910 derivatives inhibit the growth of HKe3-mutant (mt) *KRAS* spheroids.

The relative area of spheroids of HKe3-wild type (wt) *KRAS* and HKe3-mt*KRAS* treated with NP910 derivatives at day three and day six compared to that of HKe3-

wtKRAS treated with dimethyl sulfoxide (DMSO, control) at day 3. The concentration of NP910 derivatives was 16.6 μ M (A) or 50 μ M (B).

A



B

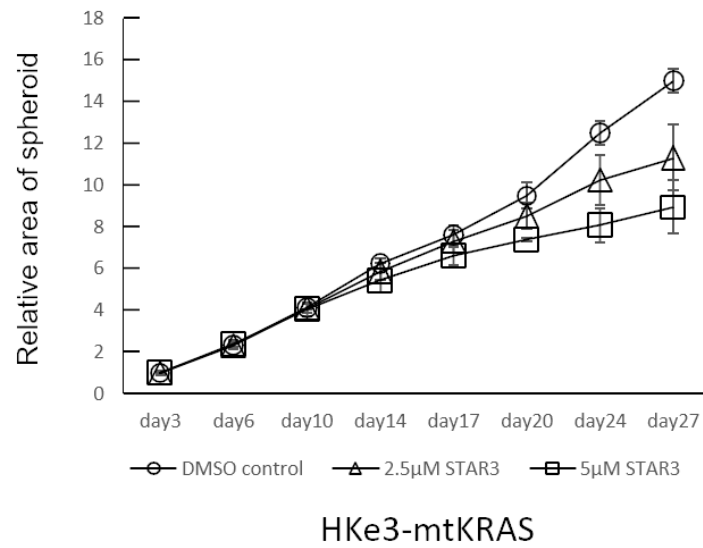


Figure 2. The long-term effect of STAR3 for HKe3-wild type (wt) *KRAS* and mutant (mt) *KRAS* spheroids A: Relative area of HKe3-wt*KRAS* spheroids treated with STAR3 from day 3 to day 27 compared to that for HKe3-wt*KRAS* treated with dimethyl sulfoxide (DMSO, control) at day 3. B: Relative area of HKe3-mt*KRAS* spheroids with STAR3 from day 3 to day 27 against HKe3-mt*KRAS* with dimethyl sulfoxide (DMSO) control at day 3.

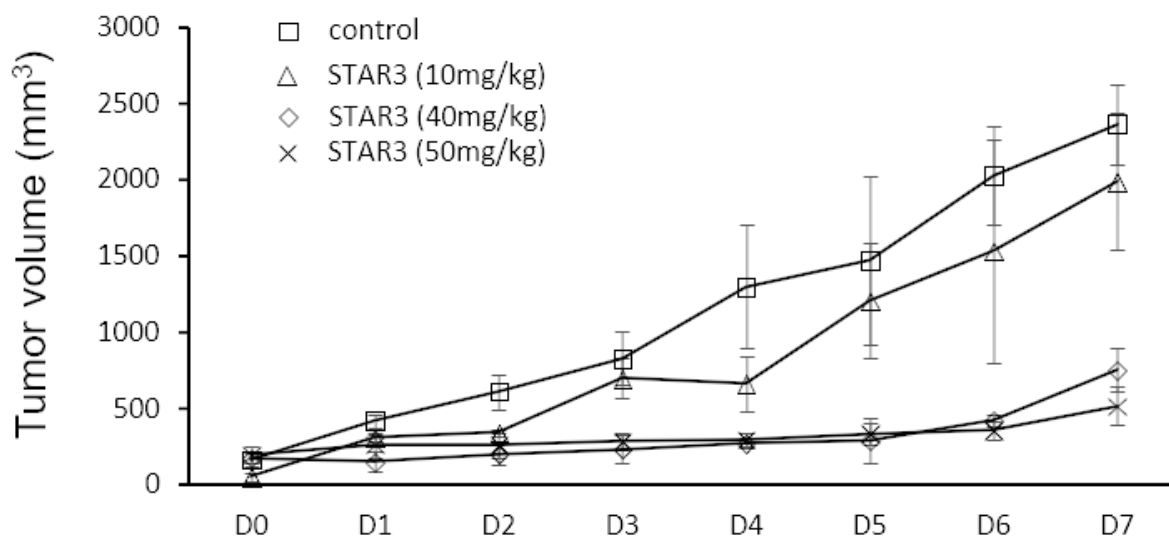


Figure 3. Effect of STAR3 on the *in vivo* tumorigenicity of human colorectal cancer HCT116 cells. HCT116 cells were injected subcutaneously into the flanks of nude mice. Relative tumour volumes are shown for mice treated with and without STAR3.

Tables

Table 1. List of NP910 derivatives.				
Name	Structure	Formula	M.W.	Distance
NP910		$C_{19}H_{29}NO_3$	319.44	0
NP674		$C_{21}H_{33}NO_3$	347.5	0.037
NP770		$C_{21}H_{33}NO_3$	347.5	0.059
NP677		$C_{23}H_{39}NO_3$	401.59	0.072
NP716		$C_{19}H_{31}NO_4$	337.46	0.135
NP917		$C_{23}H_{35}NO_5$	405.53	0.157
NP862		$C_{28}H_{40}N_2O_3$	416.6	0.186
NP676		$C_{21}H_{33}NO_4$	363.5	0.223
NP678		$C_{28}H_{37}NO_4$	427.58	0.236

NP882		$C_{27}H_{37}NO_4$	427.58	0.24
NP813		$C_{23}H_{37}NO_6$	423.55	0.241
NP842		$C_{28}H_{41}NO_4$	455.64	0.265
NP919		$C_{28}H_{34}ClNO_4$	460.01	0.288
NP713		$C_{18}H_{29}NO_3S$	351.51	0.294
NP1056		$C_{23}H_{30}FNO_3$	387.49	0.295
NP918		$C_{24}H_{35}NO_4$	401.55	0.315
NP715		$C_{21}H_{34}N_2O_4$	378.51	0.353
NP909		$C_{22}H_{28}FNO_3$	373.47	0.375
NP675		$C_{24}H_{33}NO_4$	399.53	0.388

Table II. Scoring method.

Chemical name or NPD No.	M.W.	A	B	C	D	E	F	G= A+B+C+D+E+F
		The area of HKe3-mtKRAS spheroids with 16.6µM drugs at day 6 is 0-2-fold increased (2p) or 2-4-fold increased. (1p) over 4-fold increased (0p) compared to that of HKe3-wtKRAS spheroids with DMSO control at day3.	The area of HKe3-mtKRAS spheroids with 50.0µM drugs at day 6 is 0-2-fold increased (2p) or 2-4-fold increased. (1p) over 4-fold increased (0p) compared to that of HKe3-wtKRAS spheroids with DMSO control at day3.	The increased ratio of HKe3-mtKRAS with 16.6µM drugs from Day3 to day6. 1.5 fold < increase: 0 p , 1.1 ~ 1.5fold increase:1 p 0~ 1.1fold increase:2 p	The increased ratio of HKe3-mtKRAS with 50.0µM drugs from Day3 to day6. 1.5 fold < increase: 0 p , 1.1 ~ 1.5fold increase:1 p 0~ 1.1fold increase:2 p	The increased ratio of HKe3-wtKRAS with 16.6µM drugs from Day3 to day6. 1.5 fold < increase: 2p, 1.1~ 1.5fold increase:1p 0 ~ 1.1fold increase:0p	The increased ratio of HKe3-wtKRAS with 50.0µM drugs from Day3 to day6. 1.5 fold < increase: 2p, 1.1~ 1.5fold increase:1p 0 ~ 1.1fold increase:0p	Total:12p
NP910	319.44	0	2	0	0	1	0	3
NP674	347.5	1	1	1	2	1	1	7
NP770	347.5	1	2	1	2	1	0	7
NP677	401.59	0	0	0	0	1	1	2
NP716	337.46	0	1	1	1	1	2	6
NP917	405.53	1	2	1	2	0	0	6
NP862	416.6	1	1	1	1	1	1	6
NP676	363.5	1	2	0	1	2	2	8
NP678	427.58	0	1	0	1	1	1	4
NP882	439.6	2	2	2	0	1	1	8
NP813	423.55	1	2	1	1	1	2	8
NP842	455.64	0	0	0	0	1	1	2
NP919	460.01	1	2	0	1	1	1	6
NP713	351.51	0	1	0	0	1	1	3
NP1056	387.49	0	1	0	0	1	1	3
NP918	401.55	1	2	0	2	1	1	7
NP715	378.51	1	2	1	2	1	1	8
NP909	373.47	0	1	0	0	1	1	3
NP675	399.53	1	1	1	2	2	0	7

Table 3. The effect of STAR3 in several cell lines with or without KRAS mutation

Tissue	Cell line	Type of RAS mutation	Other sequence variations (ExSPASy)	The effect of STAR3
colorectal	HCT 116	KRAS(G13D)	ACVR2A, BRCA2, CDKN2A, CTNNB, EP300, PIK3CA, TGFBR2	positive
colorectal	HKe3- mtKRAS	KRAS(G13D)	ACVR2A, BRCA2, CDKN2A, CTNNB, EP300, PIK3CA, TGFBR2	positive
colorectal	DLD-1	KRAS(G13D)	ACVR2A, APC, B2M, EP300, PIK3CA, TGFBR2, TP53	negative
colorectal	SW 620	KRAS(G12V)	APC, TP53	positive
colorectal	SW 837	KRAS(G12C)	APC, FBXW7, TP53	negative
lung	A549	KRAS(G12S)	STK11	negative
pancreas	MIA PaCa2	KRAS(G12C)	CDKN2A, TP53	positive
pancreas	Hs 766T	KRAS(Q61H)	SMAD4	positive (high conc)
liver	Hep G2	NRAS(Q61L)	TERT	positive
endometrium	HEC-1-B	KRAS(G12D)	TP53	negative
colorectal	CCK-81	WT	FBXW, PIK3CA, TP53	negative
pancreas (meta)	Hs 700T	WT	TP53	negative
melanoma	SK-MEL-28	WT	BRAF, CDK4, EGFR, PTEN, TERT, TP53	positive
kidney	A-498	WT	VHL	positive
prostate	DU145	WT	CDKN2A, RB, STK1, TP53	negative
breast	MCF-7	WT	CDKN2A, PIK3CA	negative
cervix	HeLa	WT		positive
ovarian	Caov-3	WT	TP53	negative